GENOMICS 23, 211–222 (1994)

An Ordered *Not*I Fragment Map of Human Chromosome Band 11p15

M. J. HIGGINS,[1,*] N. J. SMILINICH,[1] S. SAIT,[1] A. KOENIG,[2] J. PONGRATZ,[2] M. GESSLER,[2,3] C. W. RICHARD III,[4] M. R. JAMES,[5] J. P. SANFORD,[1] B.-W. KIM,[1] J. CATTELANE,[1] N. J. NOWAK,[1] A. WINTERPACHT,[6] B. U. ZABEL,[6] D. J. MUNROE,[7] E. BRIC,[7] D. E. HOUSMAN,[7] C. JONES,[8] Y. NAKAMURA,[9] D. S. GERHARD,[10] AND T. B. SHOWS[1]

[1]*Department of Human Genetics, Roswell Park Cancer Institute, Buffalo, New York 14263;* [2]*Institut für Humangenetik, Phillipps-Universität, D-35037 Marburg, Germany;* [3]*Theodor-Boveri-Institut für Biowissenschaften, D-97074 Wuerzburg, Germany;* [4]*Department of Psychiatry, University of Pittsburgh, Pittsburgh, Pennsylvania 15213;* [5]*INSERM U358 and Centre d'Etude du Polymorphisme Humain, Paris, France;* [6]*Universitätkinderklinik Mainz, D-6500, Mainz, Germany;* [7]*Center for Cancer Research, Massachusetts Institute of Technology, Cambridge, Massachusetts 02139;* [8]*Eleanor Roosevelt Institute, Denver, Colorado 80262;* [9]*Division of Biochemistry, Cancer Institute, Tokyo, Japan; and* [10]*Department of Genetics, Washington University School of Medicine, St. Louis, Missouri 63110*

Received March 28, 1994; revised June 16, 1994

An ordered *Not*I fragment map containing over 60 loci and encompassing approximately 17 Mb has been constructed for human chromosome band 11p15. Forty-two probes, including 11 *Not*I-linking cosmids, were subregionally mapped to 11p15 using a subset of the J1-deletion hybrids. These and 23 other probes defining loci previously mapped to 11p15 were hybridized to genomic DNA digested with *Not*I and 5 other infrequently cleaving restriction enzymes and separated by pulsed-field gel electrophoresis. Thirty-nine distinct *Not*I fragments were detected encompassing approximately 85% of the estimated length of 11p15. The predicted order of the gene loci used is cen–MYOD1–PTH–CALCA–ST5–RBTN1–HPX–HBB–RRM1–TH/INS/IGF2–H19–CTSD–MUC2–DRD4–HRAS–RNH–tel. This map will allow higher resolution mapping of new 11p15 markers, facilitate positional cloning of disease genes, and provide a framework for the physical mapping of 11p15 in clone contigs.

INTRODUCTION

Chromosome band 11p15 covers an estimated 20 Mb of DNA, contains an unusually high number of mapped genes (11p15.5 in particular), is very GC-rich, and, similar to other telomeric bands, exhibits a frequency of chiasmata higher than that of more proximal bands (Junien and Van Heyningen, 1991; Holmquist, 1992). This region is associated with a number of disease loci and contains two or more genes regulated by genomic imprinting.

Band 11p15 contains genes involved in Beckwith–Wiedemann syndrome (BWS) and tumor suppression. BWS, an overgrowth and cancer predisposition syndrome (Wiedemann, 1964, 1983), has been mapped to this region by the association of cytogenetic abnormalities such as duplications in the distal part of chromosome 11 (Waziri *et al.*, 1983; Turleau *et al.*, 1984; Aleck *et al.*, 1985) and apparently balanced chromosomal translocations and inversions in BWS patients (Mannens *et al.*, 1991; Norman *et al.*, 1992; Weksberg *et al.*, 1993a; Sait *et al.*, 1994). Linkage analysis (Koufos *et al.*, 1989; Ping *et al.*, 1989) of familial cases of BWS have mapped a disease locus near HRAS, INS, and D11S12, all of which map to 11p15.5. Loss of heterozygosity (LOH) studies of the childhood tumors associated with BWS and their sporadic counterparts demonstrate a consistent loss of alleles in 11p15, with the shortest region of overlap for rhabdomyosarcoma and Wilms tumor being D11S12 to pter (Scrable *et al.*, 1987; Coppes *et al.*, 1992). Significantly, several adult tumors, including breast cancer and bladder, testicular, and ovarian carcinoma (reviewed in Seizinger *et al.*, 1991), also exhibit LOH in this same region, which has now been named multiple tumor associated chromosome region 1 (MTACR1). Further support for the existence of a tumor (growth) suppressor gene(s) in 11p15 comes from chromosome transfer experiments in rhabdomyosarcoma and rhabdoid tumor cell lines (Dowdy *et al.*, 1991; Loh *et al.*, 1992; Koi *et al.*, 1993).

Pedigree analysis has mapped three other disease loci to chromosome band 11p15. Long QT, characterized by ventricular arrhythmias resulting in recurrent fainting and sudden death, has been genetically linked

* To whom correspondence should be addressed at Roswell Park Cancer Institute, Elm and Carlton Streets, Buffalo, NY 14263. Telephone: (716) 845-3582. Fax: (716) 845-8449.

0888-7543/94 $6.00

to HRAS in 11p15.5 (Keating *et al.*, 1991). Usher syndrome 1C (deafness, vestibular dysfunction, and progressive pigmentary retinopathy) and familial hyperinsulinism exhibit close genetic linkage with markers in 11p14–p15.1 (Smith *et al.*, 1992; Glaser *et al.*, 1994).

An increasingly large body of evidence indicates that genomic imprinting is operating in 11p15. For BWS, several observations support this conclusion (reviewed in Puech *et al.*, 1992). For example, expression of the disease appears to be determined by the sex of the transmitting parent, as evidenced by an excess of female carriers in familial BWS (Koufos *et al.*, 1989) and several examples of the transmission of 11p15 translocations and inversions to affected offspring from phenotypically normal mothers (Mannens *et al.*, 1991; Norman *et al.*, 1992; Christian *et al.*, 1993; Weksberg *et al.*, 1993a). Furthermore, uniparental disomy for 11p15.5 markers has been demonstrated in some sporadic cases of BWS (Henry *et al.*, 1991). While other explanations exist, the specific loss of maternal 11p15 alleles in pediatric tumors is also consistent with genomic imprinting (Seizinger *et al.*, 1991). Genomic imprinting has been implicated in HLA-DR4-dependent diabetes susceptibility (Julier *et al.*, 1991), a condition that maps at or very close to the INS/IGF2 locus. Two 11p15.5 genes, IGF2 and H19, have been shown to be oppositely imprinted (Zhang and Tycko, 1992; Giannoukakis *et al.*, 1993; Ogawa *et al.*, 1993; Ohlsson *et al.*, 1993; Rainier *et al.*, 1993). Disruption of the imprinting of IGF2, and perhaps H19, has been demonstrated in BWS patients and in Wilms tumor (Weksberg *et al.*, 1993b; Ogawa *et al.*, 1993; Rainier *et al.*, 1993). It remains to be shown whether additional genes in 11p15 exhibit monoallelic expression.

To identify and to clone genes involved in the diseases described above and to characterize and to study a genomic imprinted domain in humans, high-resolution maps of 11p15 are needed. Positional cloning of disease loci can benefit from a variety of 11p15 maps. A large number of new polymorphic markers have recently been identified (Takiia *et al.*, 1992; Weissenbach *et al.*, 1992; Couillin *et al.*, 1994), which will facilitate the construction of a high-resolution genetic map (O'Rahilly *et al.*, 1992; NIH/CEPH Collaborative Mapping Group, 1992; Litt *et al.*, 1993; Gyapay *et al.*, 1994). Large numbers of other probes have been generated and mapped within 11p15, and ordered clone maps are under way (Glaser *et al.*, 1989; Harrison-Lavoie *et al.*, 1989; Newsham *et al.*, 1991; Heding *et al.*, 1992; Puech *et al.*, 1992). Most recently, a high-resolution radiation hybrid map has been constructed for the region (Richard *et al.*, 1993; James *et al.*, 1994). We have developed an ordered *Not*I restriction fragment map of 11p15. The map consists of 39 *Not*I fragments encompassing close to 17 Mb of DNA and contains over 60 loci. The high-resolution framework provided by this map will allow expedient localization of new markers and will facilitate the positional cloning of disease genes in the region.

MATERIALS AND METHODS

Cell lines. GM00131 and GM07048 are normal human lymphoblastoid cell lines. GM00131 was used as a human control on hybrid mapping panels, while GM07048 served as the standard DNA source for pulsed-field gel electrophoresis (PFGE). Several other human lymphoblastoid (LiDa, GM01484), fibroblast (GM02718, GM02971, GM04250, GM06419), and tumor (RD, AG73, A204) cell lines were used to provide restriction site methylation variability for PFGE analysis (e.g., Fig. 5). Cell lines with names prefaced with GM were obtained from the NIGMS Human Genetic Mutant Cell Repository (Camden, NJ). RD, AG73, and A204 were purchased from the American Type Culture Collection (ATCC) (Rockville, MD). Ten hybrid cell lines from the J1-deletion panel (Kao *et al.*, 1976) contain progressively smaller segments of 11p15 (Glaser *et al.*, 1989).

DNA probes. The probes used in this study were obtained from a variety of sources (Table 1). For H19 a probe was prepared by PCR using primers designed from published sequences (Richard *et al.*, 1993). This probe was also used to retrieve a cosmid from the chromosome 11 library LA11NC01 (L. Deaven, Los Alamos National Laboratory), fragments of which were also used as H19 probes. cDNA30A and cDNA49C are cDNA clones identified in a brain frontal cortex library with cloned exons. These exons, as well as exon 34C, were isolated (D.J.M., unpublished results) using the exon amplification method of Buckler *et al.* (1991).

*Not*I-linking cosmids were identified using *Not*I end-clones constructed from hybrid J1-11 (A.K., J.P., M.G., unpublished). Inserts from pools of *Not*I-end phage clones mapping to 11p15 were hybridized to the arrayed chromosome 11 cosmid library. DNA from individual positive cosmids was digested with *Eco*RI, *Not*I, and *Eco*RI plus *Not*I to identify overlapping cosmids containing the same *Not*I site(s). *Eco*RI fragments cleaved by *Not*I were excised from low-melting-point agarose gels, radiolabeled by random priming (Feinberg and Vogelstein, 1983) and hybridized to Southern blots of *Eco*RI and *Eco*RI/*Not*I digests of genomic DNA to confirm that the *Not*I site(s) in the cosmids was cleaved in the genome.

Hybrid panel analysis. Genomic DNA (5 μg) from the J1-series cell lines, human (GM00131) and hamster (CHW1102), was digested with *Eco*RI or *Hin*dIII (New England Biolabs) using the buffers supplied. Following overnight electrophoresis in 0.8% agarose, gels were transferred to GeneScreen Plus (NEN-Dupont) under conditions recommended by the manufacturer. Hybridization was carried out in 1 *M* NaCl, 1% SDS, 10% dextran sulfate (Pharmacia), and 150 μg/ml denatured salmon sperm DNA using DNA probes labeled by random priming. Labeled DNA fragments containing repetitive sequences were precipitated with ethanol, redissolved in 7.5 mg/ml human placental DNA in 5× SSC (1× SSC is 0.15 *M* NaCl/0.015 sodium citrate, pH 7.0), boiled for 5 min, and preannealed for 15 min at 65°C.

Pulsed-field gel analysis. High-molecular-weight DNA from GM07048 (and other cell lines in some cases, e.g., Fig. 5) was prepared in agarose plugs from cells suspended in phosphate-buffered saline (10^7 cells per ml) as described (Higgins *et al.*, 1989). Restriction enzyme digests were carried out under the buffer conditions recommended by the supplier (New England Biolabs) except that spermidine was added (to a final concentration of 5 m*M*) to buffers with >50 m*M* NaCl. To ensure complete digestion with a minimum amount of enzyme, digests were set up by combining all reaction components on ice and maintaining the reaction mixtures overnight at 4°C before incubation at the appropriate temperature for 90 min. Restriction digests were routinely done using 7 units enzyme/μg DNA, except with *Sgr*AI, which was used at 4 units/μg DNA.

Pulsed-field electrophoresis was carried out using either a CHEF-DRII (BioRad, Inc.) or a one-dimensional PFGE system as described previously (Lalande *et al.*, 1987). CHEF gels were 1% agarose in 0.5× TBE (1× TBE is 89 m*M* Tris–borate/89 m*M* boric acid/2 m*M* EDTA, pH 8.3). CHEF gel switching conditions were 8 s (22 h, 200 V) for small fragments up to 200 kb, a 10- to 50-s ramp (29 h, 200 V) for fragments of 20 to 700 kb, and 60 s (17 h, 200 V) followed by 100 s (12 h, 200 V) for a wide range of separation from 20 to 1100 kb. For analysis of very large restriction fragments (i.e., >1000 kb),

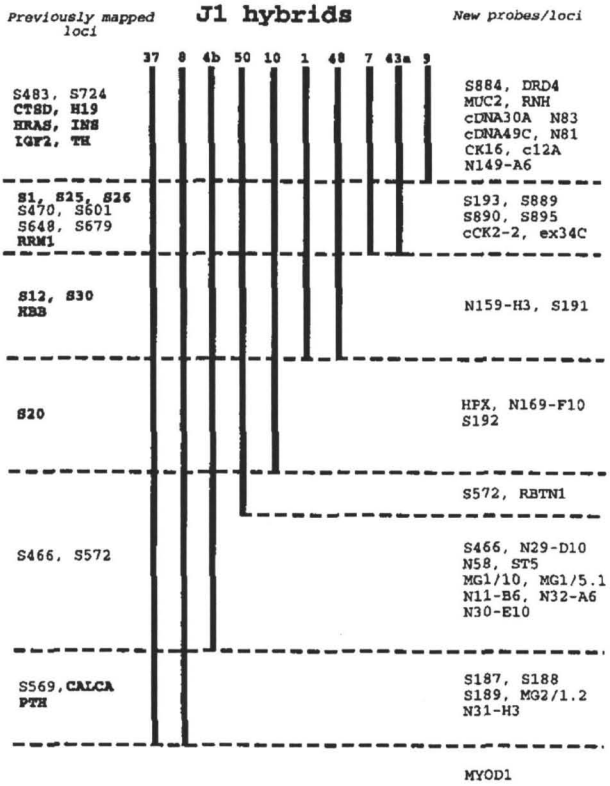

FIG. 1. The 10 J1 hybrids used in this study are shown schematically with their 11p15 content indicated by the heavy vertical lines. The loci shown to the left in boldface are those used in the original characterization of the J1 hybrids (Glaser *et al.*, 1989) with the remainder being those mapped by Tanigami *et al.* (1992). The new loci mapped using the J1 hybrids, as well as the additional mapping interval defined with J1-50, are shown to the right of the figure.

either CHEF gels were used at 120 and 180 s for 22 h each at 150 V or the one-dimensional PFG apparatus was used with switching times varying between 75 and 3000 s as described (Higgins *et al.*, 1990). Transfer of pulsed-field gels to nylon membranes and hybridization were as described above, except that before denaturation the gels were nicked for 90 s on a UV transilluminator.

Interphase fluorescence in situ hybridization. Interphase mapping was carried out on foreskin fibroblast cultures (GM08333) using the methods of Trask *et al.* (1991) and Flejter *et al.* (1993) with minor modifications.

RESULTS

Mapping using the J1 hybrids. The J1 series of deletion hybrids (Kao *et al.*, 1976) were used to establish the first physical orientation of known genes and anonymous DNA markers in chromosome band 11p15 (Glaser *et al.*, 1989). The 10 members of this hybrid panel used in the present study are shown in Fig. 1, with markers used in the original characterization indicated in boldface. With the exception of D11S20, each of the loci shown to the left in Fig. 1 has been included in the long-range mapping (see below). Originally this subset of J1 hybrids subdivided 11p15 into five distinct map intervals (Glaser *et al.*, 1989). Some of these same hybrids have been used to group several cosmids in 11p15 (Tokino *et al.*, 1991), two of which (D11S466 and D11S572) defined an additional interval between the breakpoints of J1-10 and J1-4b (Tanigami *et al.*, 1992).

We have used this set of hybrids to map more than 40 additional 11p15 markers (Fig. 1). For example, a probe for DRD4 hybridized to each member of the set, localizing it to the most distal interval with several other genes, including IGF2 and HRAS. A probe (pCRT21) for the RBTN1 gene hybridized to J1-37, J1-8, J1-4b, and J1-50 (but not to J1-10). This result localizes this locus to the same interval as D11S572, proximal to HPX, and demonstrates that J1-50 (like J1-4b) extends proximally farther than J1-10 (Fig. 1). The inclusion of J1-50 in the mapping panel located D11S466 (which is negative in this hybrid) proximal to RBTN1 and D11S572 into a new interval containing several loci, including ST5. The localization for the remainder of loci mapped using this subset of J1 hybrid is summarized in Fig. 1.

Long-range restriction mapping. A total of 65 probes (Table 1) for anonymous DNA segments, *Not*I-linking clones, and gene sequences were included in the pulsed-field gel analysis of p15. In general, each probe was hybridized to GM07048 DNA digested with *Not*I and five other infrequently cleaving restriction enzymes (Table 2). Double digests with *Not*I in combination with the other enzymes were not performed; however, results from other restriction digests provided confirmation of physical linkage, order information, and, in some cases, maximum distances between *Not*I fragments.

Initially, each probe was hybridized to Southern blots prepared from CHEF gels run under "standard" conditions chosen to separate a wide range of DNA fragments from 20 to ~1100 kb. Probes detecting restriction fragments less than 200 kb long were also hybridized to the same digests electrophoresed in an "8 s" CHEF gel, which gave much higher resolution in the 10- to 200-kb range. If no distinct band was observed for a given probe in one or more restriction digests run in the "standard" CHEF, or if there was obvious hybridization at the compression zone, then the marker was also hybridized to Southern blots prepared from CHEF gels run at 120- and 180-s switch times or one-dimensional pulsed-field gels (see Materials and Methods), which separated DNA fragments up to 6000 kb.

When establishing physical linkage, a number of criteria were observed to distinguish between identical and comigrating nonidentical restriction fragments. For example, if two loci are suspected to be physically linked based on commonality of restriction fragments, then they must be in the same or adjacent hybrid map intervals. In general, two loci were considered physically linked when their respective probes detected common fragments generated by at least two restriction

TABLE 1

Probes Used in Pulsed-Field Gel Analysis

Probe name	Locus	Source/reference
pT24C3	HRAS	ATCC[a]
phins214	INS	ATCC
phins311	IGF2	ATCC
pHGTH4	TH	ATCC
pE1.8	RRM1	ATCC
pADJ762	D11S12	ATCC
pMyf3	MYOD1	ATCC
p20.36	PTH	ATCC
D11RP633	D11S187	Davis *et al.* (1988)
D11RP789	D11S188	Davis *et al.* (1988)
D11RP890	D11S189	Davis *et al.* (1988)
D11RP1030	D11S191	Davis *et al.* (1988)
D11RP1038	D11S192	Davis *et al.* (1988)
D11RP1051	D11S193	Davis *et al.* (1988)
pCS1	D11S1	Glaser *et al.* (1989)
pγ6	D11S25	Glaser *et al.* (1989)
pGGE0.9	D11S26	Glaser *et al.* (1989)
pJ1.1	D11S30	Glaser *et al.* (1989)
pSPβc	HBB	L. Maquat, RPCI
p1215	HBB	P. Dierks, U. of Vermont
pTT24	CALCA	B. Nelkin, Johns Hopkins University
pCD2.1EX	CTSD	J. Chirgwin, U. of Texas
cC4 (76H3[b])	CTSD	B. Weissman, U. of North Carolina
p1596	ST5	J. Licky, Department of Defense
pHPX	HPX	F. Altruda, U. of Torino
Clone 20	DRD4	H.H.M. Van Tol, Clarke Institute
cM4 (83B11[b])	MUC2	B. Weissman, U. of North Carolina
cI11-280	D11S466	JCRRB[c]
cI11-289	D11S470	JCRRB
cI11-330	D11S483	JCRRB
cI11-434	D11S569	JCRRB
cI11-440	D11S572	JCRRB
cI11-555	D11S764	JCRRB
cI11-565	D11S601	JCRRB
N81, N83	—	Sanford *et al.* (1993)
pRAI	RNH	Schneider *et al.* (1988)
pB2, pCRT21	RBTN1	UK DNA Probe Bank
MG1/5.1, 1/10, 2/1.2	—	λ-clones selected with 11p15.5, microdissection library[d]
CK16	—	*Alu*-PCR clone, B.W.K., unpublished
CR133	D11S884	Richard *et al.* (1993)
CR149	D11S889	Richard *et al.* (1993)
CR154	D11S890	Richard *et al.* (1993)
CR179	D11S895	Richard *et al.* (1993)
H19-PCR	H19	Richard *et al.* (1993)
cH19	H19	See Materials and Methods
cDNA30A, 49C, and exon 34C	—	See Materials and Methods
*Not*I-linking cosmids[e]	—	See Materials and Methods

[a] American Type Tissue Collection (Rockville, MD).

[b] Plate and coordinate number in the arrayed chromosome 11 cosmid library LA11NC01 (L. Deaven, Los Alamos National Laboratory; G. Evans, Salk Institute).

[c] Japanese Cancer Research Resources Bank (Tokyo).

[d] Microdissection library provided by U. Claussen and B. Horsthemke (U. of Essen).

[e] *Not*I-linking clones are designated by the plate and coordinate number (prefaced by the letter N) in the arrayed cosmid library.

endonucleases. When possible, identity of restriction fragments was confirmed by using the same blot for the two probes in question. Probes for loci on the same restriction fragment should detect similar or complementary patterns of methylation or polymorphism-induced change in size or intensity.

Fragment sizes for each of the loci analyzed are compiled in Table 2. Thirty-nine distinct *Not*I fragments were detected with a combined length of almost 17,000 kb. The length of the fragments varied widely from 20 to 2500 kb. Although gaps exist, in many cases commonality of restriction fragments generated by other enzymes established physical linkage of loci on different *Not*I fragments. Using the hybrid mapping data and the information in Table 2, an ordered *Not*I restriction fragment map of 11p15 has been constructed (Fig. 2). The following is a description of some of its features.

The MYOD1/PTH/CALCA region. Although MYOD1 has been mapped to 11p14.3–p15.1 (Gessler *et al.*, 1990; Henry *et al.*, 1993), it was not present in either J1-8 or J-37, making it the most centromeric marker on the map. DNA probes for eight loci within the interval defined by hybrid J1-4b and hybrid pair J1-8/37 detected five different *Not*I fragments (Fig. 2A). *Not*I-linking cosmid N31-H3 detected both the 280-kb fragment detected by MG2/1.2 and the 2500-kb fragment carrying CALCA and D11S188. This linkage was verified using other restriction enzymes (Table 2) and provides the only confirmed physical connection between loci in this interval. D11S189 is contained in two independent radiation hybrids that are positive for all distal loci tested (i.e., RBTN1, HBB, D11S12, IGF2, and HRAS) but negative for CALCA, PTH, and MYOD1 (unpublished results), positioning this locus distal to CALCA and PTH. D11S569 has also been located distal to CALCA and PTH by radiation hybrid mapping (James *et al.*, 1994). A tentative linkage between D11S189, D11S569, and CALCA through a 2300-kb *Asc*I fragment supports the placement of CALCA telomeric to PTH (Henry *et al.*, 1989; O'Rahilly *et al.*, 1992).

The RBTN1/ST5 gene region. A number of probes, including four new *Not*I-linking loci, mapped into the region containing the RBTN1 and ST5 genes by virtue of their being positive in J1-4b and negative in J1-10. Of these, only D11S572 was contained in J1-50 with RBTN1 (Fig. 1). Since J1-50 was a difficult hybrid to use (because only a small proportion of cells contained human DNA), each probe in the J1-4b to J1-10 interval was also tested with somatic cell hybrids segregating the der(11) and der(14) chromosomes of a T-cell leukemia t(11;14), the chromosome 11 breakpoint that defined the RBTN1 gene (Boehm *et al.*, 1988). D11S572 segregated with the telomeric probe for RBTN1, while the remainder of the loci segregated with the centromeric RBTN1 probe (data not shown), thus confirming that RBTN1 and D11S572 are distal to the other loci in this interval.

Cosmid cDI11-280 (D11S466) detected 260- and 350-

TABLE 2

Restriction Fragments Containing 11p15 Loci

Locus	*Not*I	*Asc*I	*Bss*HI	*Sgr*AI	*Mlu*I	*Nru*I	Locus	*Not*I	*Asc*I	*Bss*HI	*Sgr*AI	*Mlu*I	*Nru*I
MYOD	40	ND	20	350	40	680	D11S25	600	440	175	330	190	200
	550			400	280		D11S26	850			525	320	400
PTH	730	2100	730	ND	730	260	D11S470				650	660	
D11S187					1150		cCK2-2				1100		
					1600		D11S890	170	160	170	170	160	680
CALCA	2500	2300	100	1800	100	1400	D11S601	60	280	60+	480		1060
D11S188				2200		2200			725				
N31-H3	2500	2300	290	1800	650	1400	D11S193	60	280	60	170	160	680
	280		250	2200		2200	D11S895		725		480		1060
MG2/1.2	280	2300	250	1800	650	400	Exon 34c						
D11S569	650	2300	320	500	ND	1000	D11S648	35	280	35	20	160	680
D11S189	1050	2300	800	1400	1125	630			725	240			1060
						700	D11S1	160	280	45	100	470	680
						1125	D11S679	180	725	90	200	550	1060
N30-E10	325	200	140	730	2300	460		430		130	360		
N155-E5	700		485								400		
			550								450		
N32-A6	700	500	220	50	450	600	D11S724	250	445	200	250	470	680
	400		450	650	2300			410	725	250	450	550	1060
			600					430		300			
N11-B6	400	500	100	100	2300	900	IGF2	280	560	25	55	125	380
N167-C4	100		200	300			INS	550	730	115	115	260	1060
			450	400			TH				205	630	
ST5	260	400	200	600	2300	900	D11S884				300	660	
MG1/5.1			260	680								780	
MG1/10							H19	280	560	210	140	140	170
N58							cDNA30a	550	730		220	380	480
D11S466	260	400	200	600	2300	900					340	480	650
N29-D10	350		260	680		460					480	630	
N57-C12												660	
RBTN1	280	1000	350	80	2300	460						780	
(B2)				680			CTSD	325	560	80	80	245	400
RBTN1	280	1000	200	280	2300	200			730	245	220	350	480
(CRT21)											270	380	650
D11S572	280	1000	200	280	195	200					340	480	
					380						450	630	
D11S192	780	600	460	1400	1100	1100					480	660	
						1800						780	
N169-F10	780	600	460	1400	1100	1800	CK16	560	1500	560	975	975	1200
	900		730								1100	1500	
HPX	900	ND	120	230	2200	150	N81	150	360	75	150	180	300
			460	1000	3400	220			650	150	175	210	500
HBB	2300	4000	1200	450	2200	370					230	250	
				550	3400	1300	N149-A6	150	360	150	150	180	300
						2100		200	650	100	230	210	500
						3100	MUC2	120	290	275	400	240	200
D11S30	2300	4000	1200	1100	2200	3100		300	650	400		290	440
					3400			400				440	520
D11S191	2300	4000	1200	1100	1350	2100		570					
					3400	3100	DRD4	60	85	60	175	180	60
N159-H3	2300	4000	250	1100	1350	1100	c12A						120
	390		350		3400	1350							200
						2100	HRAS	30	50	20	75	30	7
						3100		90				350	25
D11S12	390	2400	350	1100	470	1100						430	
		3400			660	1350						520	
		4000			1160	2100	RNH	60	225	60	75	350	350
					1350	3100		90				430	
					3400							520	
RRM1	390	3400	350	1100			N83	50	225	40	160	350	350
		4000										430	
D11S889	390	3400	350	310	470	2100						520	
		4000			660	3100	D11S483	90	50	50	ND	90	350
					1350		cDNA49c					430	
					3400								

Note. The sizes (in kilobases) of restriction fragments detected by 11p15 probes in *Not*I, *Asc*I, *Bss*HII, *Sgr*AI, *Mlu*I, and *Nru*I digests are listed. Restriction fragments that establish physical linkage are enclosed in shaded boxes. Linkages defined by only one poorly resolved fragment are shown in open boxes. ND, not determined.

kb *Not*I fragments, as well as 460- and 900-kb *Nru*I fragments (Fig. 3A, Table 2). Restriction analysis demonstrated that cCI11-280 is both a *Not*I and a *Nru*I linking clone (not shown). Probes MG1/5.1 (Fig. 3A), MG1/10, N58, and p1596 (ST5) each detected the 260-kb *Not*I and 900-kb *Nru*I fragments, as well as several other restriction fragments (Table 2) in common with cCI11-280. The two probes used for the RBTN1 locus (pCRT21 and pB2) detect the same *Not*I, *Asc*I, and *Mlu*I fragments, but different *Bss*HII and *Nru*I fragments, suggesting that a CpG-island may exist between them. The 680-kb *Sgr*AI fragment detected by pB2, the proximal RBTN1 probe, was also detected by cCI11-280. This physical linkage was supported by a

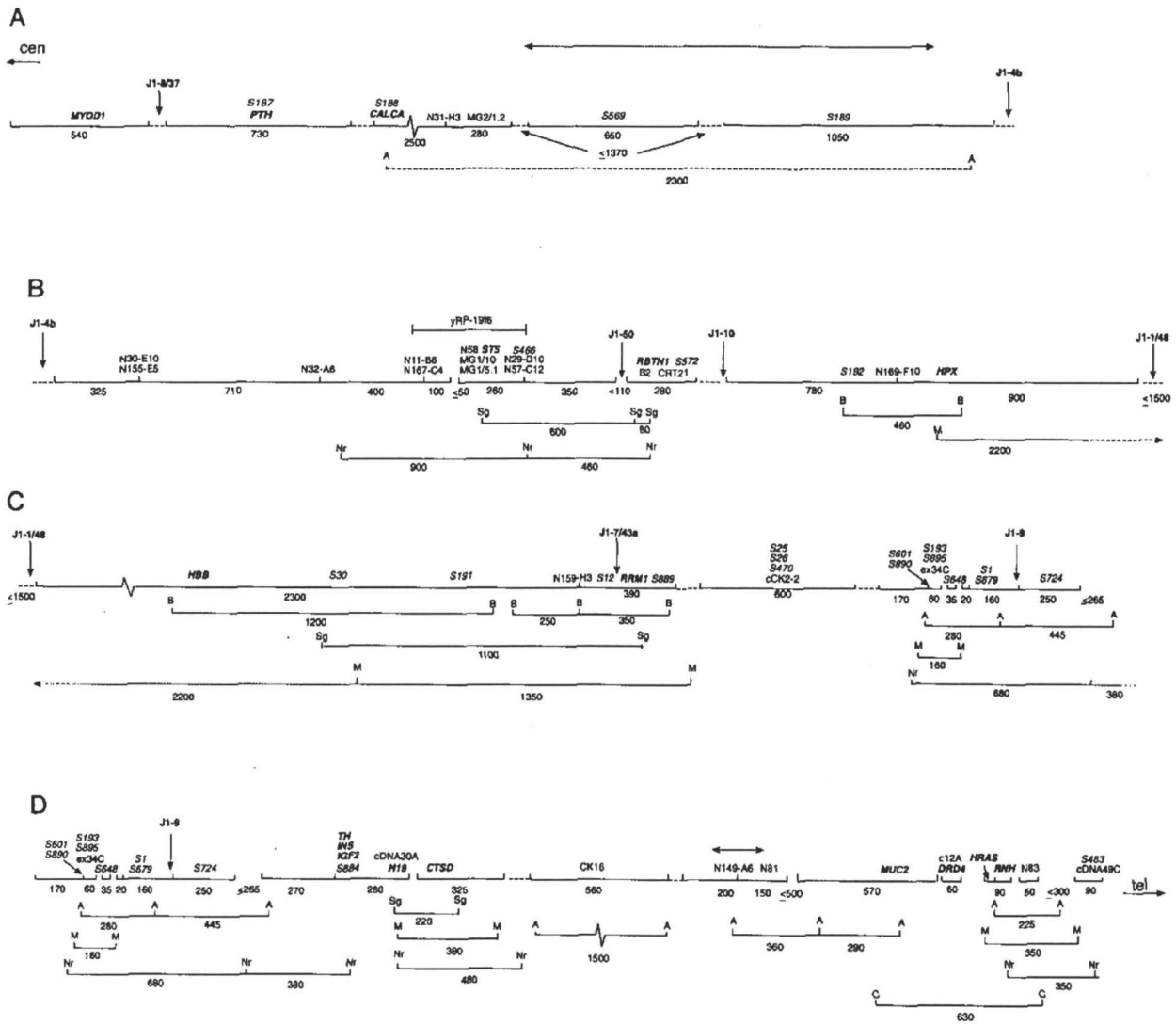

FIG. 2. Ordered *Not*I fragment map of 11p15. Only the *Not*I fragments are shown, except when those fragments generated by other enzymes allow ordering or estimation of genomic distances between *Not*I fragments. Other enzymes were *Asc*I (A), *Bss*HII (B), *Cla*I (C), *Mlu*I (M), *Nru*I (Nr), and *Sgr*AI (Sg). Probes designated by the letter "S" and then a number indicate D11S loci. The size of each *Not*I fragment is shown below the line. The 2300-kb *Asc*I fragment connecting CALCA/D11S188 and D11S189 is drawn as a dashed line to indicate that physical linkage between these loci is based solely on this single restriction fragment and, therefore, remains tentative. Ambiguity in the order of fragments is indicated by the arrows above the map. The positions of the breakpoints of the J1 hybrids are indicated by the vertical arrows. Their placement is only approximate, and it is not necessarily implied that they disrupt the *Not*I fragment drawn below. The total length of DNA mapped as *Not*I fragments is approximately 17 Mb or about 85% of the estimated length of 11p15.

460-kb *Nru*I fragment in common between these two loci (Fig. 3) and positions D11S466 and the ST5 gene just centromeric of RBTN1 (Fig. 2B). From this result, the gap between *Not*I fragments carrying RBTN1 and D11S466 was estimated to be ≤110 kb. The 900-kb *Nru*I fragment containing D11S466 MG1/5.1, MG1/10, N58, and ST5 was also detected by *Not*I-linking cosmids N11-B6 and N167-C4 (Table 2). This linkage was confirmed by the finding that probes from N11-B6 and cCI11-280 detected a 400-kb YAC (yeast artificial chromosome) in common (unpublished result). N11-B6 (and N167-C4) represents one *Not*I site in a 1535-kb contiguous map consisting of four *Not*I fragments just centromeric to the ST5 gene (Fig. 2B) defined entirely by *Not*I-linking cosmids. No restriction fragments were found in common between N30-E10/N155-E5 and either D11S189 or D11S569, precluding an estimation of the genomic distance separating them.

The HPX gene region. Probes for D11S192, N169-F10, and HPX were positive in J1-10 but negative in hybrid pair J1-1/48, placing these three loci between RBTN1 and HBB (Fig. 1). The *Not*I site-containing

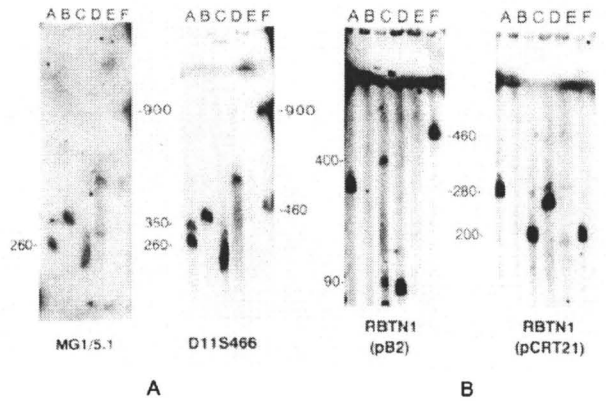

FIG. 3. Pulsed-field gel analysis of loci in the RBTN1 gene region. High-molecular-weight DNA from cell line GM07048 was digested with *Not*I (lane **A**), *Asc*I (lane **B**), *Bss*HII (lane **C**), *Sgr*AI (lane **D**), *Mlu*I (lane **E**), and *Nru*I (lane **F**) and electrophoresed in CHEF gels. Switching times were either 60 s followed by 100 s (**A**) or a 10- to 50-s ramp (**B**). Following transfer to nylon membranes, the filters were hybridized with probes for the indicated loci. The sizes of selected fragments are in kilobases.

fragment from N169-F10 detected 780- and 900-kb *Not*I fragments. LL1038 (D11S192) detected the 780-kb *Not*I fragment and other fragments in common with N169-F10, while a probe for HPX detected the 900-kb *Not*I fragment and *Bss*HII fragments identified by this *Not*I-linking cosmid (Table 2). The orientation of these three loci is uncertain; however, tentative linkage of HPX to HBB through two large (2200 and 3400 kb) *Mlu*I fragments places the 900-kb *Not*I fragment distal to the 780-kb fragment (Fig. 2B). No physical connections between D11S192, N169-F10, or HPX have been established with D11S572 and RBTN1 in the next centromeric hybrid mapping interval.

The HBB/D11S12 interval. Five loci were positive for hybrid pair J1-1/48 but missing in hybrid pair J1-7/43a (Fig. 1). Three of these (D11S30, D11S191, HBB) lie on a 2300-kb *Not*I fragment, while D11S12 was contained on a 390-kb *Not*I fragment (Fig. 4, Table 2). The *Not*I-linking fragment from N159-H3 detected both the 2300- and the 390-kb fragments (Fig. 4), demonstrating that these two *Not*I fragments are contiguous (Fig. 2C). Several large restriction fragments (*Asc*I, *Mlu*I, *Nru*I) appear to be in common between D11S12 and the HBB group of loci (Fig. 4, Table 2). However, HBB does not share a 1100-kb *Sgr*AI fragment in common between D11S12, N159-H3, D11S191, and D11S30, making it the most proximal of these markers. The detection of a 2200-kb *Mlu*I fragment by pJ1.1 (D11S30) rather than the 1350-kb *Mlu*I fragment detected by LL1030 (D11S191), N159-H3, and pADJ762 (D11S12) positions D11S30 centromeric to the other three loci (Fig. 2C).

The J1-7/43a to J1-9 interval. Eight loci used in this analysis have been mapped previously (Glaser *et al.*, 1989; Tanigami *et al.*, 1992) into the region delimited by the 11p15 breakpoints of J1-7/43a and J1-9 (i.e., between D11S12 and the gene cluster containing TH, INS, IGF2, CTSD, and H19). Six additional loci have been located in this interval (Fig. 1). Probes for RRM1 and D11S889 hybridized to most of the same restriction fragments as D11S12. Since D11S12 is absent from J1-7/43a, it must be centromeric to RRM1 and D11S889. RRM1 also lies on the 1100-kb *Sgr*AI fragment in common between D11S12, N159-H3, D11S191, and D11S30. Since the probe for D11S889 detects a 310-kb *Sgr*AI fragment instead, it must be telomeric to both RRM1 and D11S12.

The remaining loci in this interval define seven more *Not*I fragments ranging from 20 to 600 kb (Fig. 2C). Unexpectedly, probes for four independently cloned loci (D11S25, S26, S470, cCK2-2) detected a 600-kb *Not*I fragment and exactly the same set of restriction fragments with each of the other enzymes used, the smallest being a 170-kb *Bss*HII fragment. Thus, no order could be inferred. The cosmid cCI11-565 (D11S601) contains restriction sites for *Not*I, *Asc*I, and *Bss*HII and, typical of linking clones, detects two restriction fragments for each of these enzymes (three in *Asc*I). D11S193, D11S895, and exon 34C are located on the smaller (60 kb) of the two *Not*I fragments defined by D11S601. In contrast, pCS1 (D11S1) and cCI11-469 (D11S679) contain none of these restriction sites yet hybridize to three *Not*I fragments and three *Bss*HII fragments (Table 2). Variability in the detection of these fragments in DNA samples from different cells (data not shown) indicates that these multiple bands are due to incomplete methylation at restriction sites. *Not*I partial digest fragments detected by pCS1 and cCI11-469 are also detected by cCI11-555 (D11S724), the most proximal locus in the next (J1-9) hybrid interval. Thus, the 11p15 breakpoint in J1-9 is between

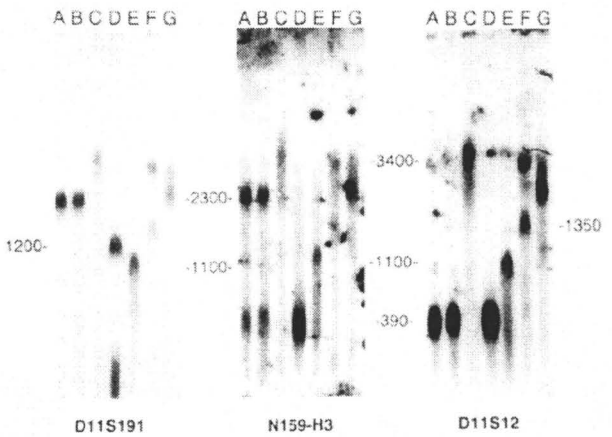

FIG. 4. Long-range restriction mapping of loci in the J1-1/48 to J1-7/43a interval. *Not*I (lane **A**), *Asc*I (lane **B**), *Bss*HII (lane **C**), *Sgr*AI (lane **D**), *Mlu*I (lane **E**), and *Nru*I (lane **F**) digests of GM07048 were separated in a one-dimensional PFGE system (see Materials and Methods), transferred to GeneScreen Plus, and hybridized with probes for the indicated loci. The *Not*I-linking cosmid N159-H3 detected both the 2300-kb *Not*I fragment containing D11S191 and the 390-kb *Not*I fragment detected by pADJ762 (D11S12). Sizes are in kilobases.

D11S1/D11S679 and D11S724. These three loci were also physically linked to each other and to D11S648, exon 34C, D11S895, D11S193, D11S601, and D11S890 through two adjacent *Asc*I fragments (Fig. 2C).

The J1-9 interval. The most telomeric region defined by the J1-hybrids was shown to contain several genes, including HRAS, INS, IGF2, TH, CTSD, and H19 (Glaser *et al.*, 1989). Three additional genes, MUC2, DRD4, and RNH, have now been mapped to this interval (Fig. 1). Analysis of overlapping clones has shown that IFG2 and INS are less than 13 kb apart (Bell *et al.*, 1985), and linkage analysis has placed TH very close to these loci (Moss *et al.*, 1986; Xue *et al.*, 1988). Not surprisingly, probes for each of these loci detected exactly the same set of restriction fragments, including a 25-kb *Bss*HII fragment (Table 2). A probe for CTSD detected two *Asc*I fragments and three *Mlu*I fragments in common with IGF2 but was found to be on a different *Not*I fragment (Table 2). Probes for the H19 gene detected the same *Not*I fragments as IGF2/INS/TH but *Sgr*AI and *Nru*I fragments in common with CTSD, indicating that H19 is between IGF2 and CTSD. The orientation of these three loci was determined by the analysis of *Nru*I partial-digest fragments, which demonstrated physical linkage of IGF2 to the more proximal marker D11S1. Since *Nru*I was the only enzyme that connected IGF2 with D11S1, multiple DNA samples were examined to eliminate the possibility that D11S1 and IGF2 are contained on different comigrating fragments. pCS1 (D11S1) detected 680- and 1060-kb *Nru*I fragments with relative intensities that varied among DNA samples (Fig. 5). phins311 (IGF2) detected 380- and 1060-kb fragments with the same variability in intensity. Furthermore, since the combined length of the two smaller *Nru*I fragments (380 + 680) is the same as that of the common partial digest products, these results prove that the 1060-kb fragment detected by D11S1 and IGF2 probes is the same. A similar experiment was carried out to confirm the linkage of H19 and CTSD through 480- and 650-kb *Nru*I fragments (Fig. 5 and data not shown). The order of the four loci used in this analysis is therefore cen–D11S1–IGF2–H19–CTSD–tel.

Linkage analysis has shown that HRAS is distal to TH/INS/IGF2 (Moss *et al.*, 1986; O'Rahilly *et al.*, 1992). We have previously demonstrated close physical linkage of the RNH gene to HRAS (Schneider *et al.*, 1992). A radiation hybrid, which was found to be positive for HRAS, RNH, and a putative telomere probe (Cheng *et al.*, 1989) but negative for CTSD, H19, IGF2, and more centromeric 11p15 loci, allowed the subdivision of the remaining J1-9 positive loci (Fig. 1) into two groups. Cosmid 12A, DRD4, N83, cDNA49C, and cCI11-330 (D11S483) were also contained in this hybrid (unpublished result), grouping them with HRAS and RNH at the telomeric end of J1-9. On the other hand, coincidence clone CK16, *Not*I-linking cosmid N149-A6, and MUC2 were not contained in this hybrid and are therefore located between CTSD and the more telomeric cluster of loci. cCI11-330, N83, and cDNA49C detected a 350-kb *Nru*I fragment in common with RNH, locating these three loci on the same side of HRAS as RNH (Table 2, Fig. 2D). The *Mlu*I restriction pattern confirmed the physical linkage and suggests that D11S483 and cDNA49C are the farthest markers in this group from HRAS. This interpretation was supported by the finding of a 630-kb *Cla*I fragment (not included in Table 2) in common among MUC2, HRAS, RNH, and N83 but not D11S483 and cDNA49C (Fig. 2D). Furthermore, since MUC2 is proximal to these loci, this result positions D11S483 and cDNA49C as the most telomeric loci in the map (Fig. 2D), a conclusion supported by interphase FISH (results not shown).

Since DRD4 and c12A are also contained within the 630-kb *Cla*I fragment but are not present on the *Mlu*I and *Nru*I fragments in common with HRAS, RNH, N83, and D11S483, these two loci must be proximal to HRAS. Interphase FISH places c12A proximal to HRAS (not shown), supporting this interpretation. A

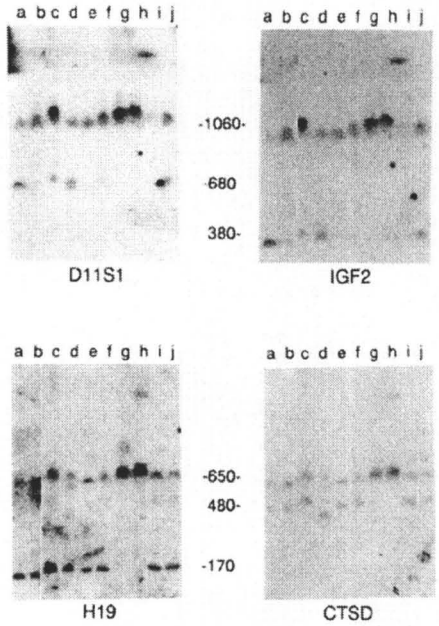

FIG. 5. Orientation of IGF2, H19, and CTSD by *Nru*I site methylation analysis. DNA from 10 cell lines was digested with *Nru*I and electrophoresed in CHEF gels using switching times of 120 and 180 s (D11S1 and IGF2) or 60 and 100 s (H19 and CTSD). Of the three loci known to be positive in J1-9 (IGF2, H19, CTSD), only IGF2 was physically linked to the more centromeric locus D11S1. The 1060-kb partial *Nru*I fragments detected by probes corresponding to D11S1 and IGF2 are the same. This conclusion is based on the similarity in the size of the partial digest fragment with the sum of the two smaller complete digest fragments (380 + 680 kb) and consistency in the relative intensities of the complete and partial digests among different DNA samples (**a–j**). Since H19 and CTSD lie on none of the three *Nru*I fragments carrying D11S1 and IGF2, these two genes are telomeric to IGF2. DNA samples were from GM07048 (**a**), GM06419 (**b**), GM01484 (**c**), GM02718 (**d**), GM02971 (**e**), GM04250 (**f**), RD (**g**), AG73 (**h**), A204 (**i**), and LiDa (**j**). Sizes are in kilobases.

probe for the MUC2 locus hybridized to several *Not*I fragments, the largest of which is 570 kb. Analysis of *Not*I digests of several different DNA samples suggests that these multiple fragments are due to incomplete digestion (probably due to restriction site methylation) rather than to cross-hybridization to homologous loci. A 650-kb *Asc*I fragment with a partially cleaved internal site connected MUC2 with the *Not*I-linking cosmid N149-A6, which detected two additional *Not*I fragments of 150 and 200 kb (Table 2). Finally, one additional *Not*I fragment of 560 kb was detected by coincidence clone CK16. This fragment is not identical to the largest fragment containing MUC2 since smaller *Not*I fragments were not observed and CK16 did not detect any other fragments in common with MUC2 (Table 2). CK16 detected a 1500-kb *Asc*I fragment and large *Sgr*AI, *Mlu*I, and *Nru*I fragments, indicating a minimum separation of 1500 kb between CTSD and the cluster of linked loci at the telomeric end of the map (Fig. 2D).

DISCUSSION

We have constructed an ordered *Not*I fragment map of chromosome band 11p15. The map consists of 65 loci contained within 39 different *Not*I fragments with a total length approaching 17 Mb. These loci have been ordered within eight intervals defined by J1-deletion hybrids. Cytogenetically, band 11p15 accounts for approximately one-third of the total length of the short arm of chromosome 11[ca. 60 Mb (Morton, 1991)]. Thus, the *Not*I fragments identified in this study constitute 85% of the estimated 20 Mb of this band.

As well as adding many new markers, the *Not*I map has refined the order of several genes and anonymous DNA markers within the J1-deletion hybrid intervals (Glaser *et al.*, 1989). The DRD4, MUC2, and RNH genes were assigned to the most telomeric (J1-9) region originally shown to contain HRAS, INS, IGF, TH, CTSD, and H19. Except for the TH/INS/IGF2 gene cluster, long-range restriction mapping has allowed ordering of these genes (Fig. 2). D11S1 has been positioned telomeric to D11S25 and D11S26 within the next proximal hybrid interval, which were located distal to RRM1. Similarly, D11S30 has been mapped to the same large *Not*I fragment as HBB but is located distal to this locus. Three new genes have been mapped between HBB and CALCA/PTH with HPX being most telomeric, followed by RBTN1 and then ST5. Tentative physical linkage of CALCA to D11S569 through a single large restriction fragment (*Asc*I) supports the placement of CALCA telomeric to PTH as determined by mitotic deletion mapping and a recent genetic linkage analysis (Henry *et al.*, 1989; O'Rahilly *et al.*, 1992), which is in contrast to the reverse order determined by earlier genetic linkage studies (Bonaïti-Pellié *et al.*, 1986) and radiation hybrid mapping (Richard *et al.*, 1993). MYOD1 was not included in the initial mapping studies using the J1-hybrids (Glaser *et al.*, 1989) but was more recently mapped proximal to J1-10 in an interval containing RBTN1, CALCA, and PTH (Henry *et al.*, 1993). In the present study MYOD1 was negative in both J1-8 and J1-37, mapping it centromeric to these genes.

The order of HRAS and DRD4 has also been in question since opposite orientations have been inferred in two different multipoint linkage analyses (Gelernter *et al.*, 1992; Petronis *et al.*, 1993). DRD4 was located proximal to HRAS by both restriction mapping (Fig. 2) and interphase FISH. No other discrepancies exist between the order of loci depicted in Fig. 2 and the published genetic linkage and radiation hybrid maps.

Although many physical linkages have been made, a number of discontinuities still exist in the map. The high density of CpG islands in the region accounts for some of these gaps by reducing the possibility of finding restriction fragments in common between adjacent loci. Assuming that 1 cR is equal to 51 kb, the radiation hybrid map of 11p15 (Richard *et al.*, 1993; James *et al.*, 1994) predicts that the majority of the gaps in the map shown in Fig. 2 are a few hundred kilobases or less. The radiation map does, however, suggest that several megabases may exist between the *Not*I fragments detected by N30-E10/N155-E5 and D11S569 and between PTH/CALCA and MYOD1 (see Fig. 2A). Additional probes in these regions and partial digest analysis will be necessary to close these gaps in the map.

The *Not*I map presented in Fig. 2 and the new probes used to construct it should provide useful reagents for the positional cloning of 11p15 disease-related genes. For example, probes for selected loci on the map have been used in FISH and PFGE analysis to map more precisely three BWS chromosome rearrangements and a rhabdoid tumor translocation between D11S1/D11S469 and IGF2 (Sait *et al.*, 1994) (see Fig. 2D). It is notable that the mapping of H19 distal to IGF2 precludes this putative tumor suppressor gene (Hao *et al.*, 1993) from being directly affected by these four rearrangement breakpoints as well as locates this gene outside of the smallest LOH region determined in breast tumors (Winqvist *et al.*, 1993). In the most telomeric portion of the map, the ordering of several new loci closely linked to HRAS provides additional markers to facilitate the identification of the gene responsible for Long QT syndrome. This map will also provide ordered sets of markers in the vicinity of IGF2 and H19 to help define and characterize an imprinted domain. Finally, in conjunction with the radiation and genetic linkage maps, this map provides many new anchor loci to aid in the construction of clone contigs of 11p15.

ACKNOWLEDGMENTS

The following persons kindly provided DNA probes used in this study: L. Maquat, P. Dierks, B. Nelkin, J. Chirgwin, B. Weissman, J. Lichy, F. Altruda, and H. Van Tol. We also thank L. Deaven for the chromosome 11 cosmid library, U. Claussen and B. Horsthemke for the microdissection library, Peter Mayers for computer graphics,

and Nancy Frame for the excellent preparation of the manuscript. This work has been supported by HG00359.

REFERENCES

Aleck, K., Williams, J., Mongkolsmai, C., Knight, S., and Taysi, K. (1985). Partial trisomy 11p with interatrial septal aneurysm: Case report and literature review. *Ann. Genet.* **28:** 102–106.

Bell, G. I., Gerhard, D. S., Fong, N. M., Sanchez-Pescador, R., and Rall, L. B. (1985). Isolation of the human insulin-like growth factor genes: Insulin-like growth factor II and insulin genes are contiguous. *Proc. Natl. Acad. Sci. USA* **82:** 6450–6454.

Boehm, T., Baer, R., Lavenir, I., Forster, A., Waters, J. J., Nacheva, E., and Rabbitts, T. H. (1988). The mechanism of chromosomal translocation t(11;14) involving the T-cell receptor Cγ locus of human chromosome 14q11 and a transcribed region of chromosome 11p15. *EMBO J.* **7:** 385–394.

Bonaïti-Pellié, C., Martinez, M., and Clerget-Darpoux, F. (1986). Multilocus linkage analysis of markers located on the short arm of chromosome 11. *Genet. Epidemiol.* (Suppl.) **1:** 129–134.

Buckler, A., Chang, D. D., Graw, S. L., Brook, J. D., Haber, D. A., Sharp, P. A., and Housman, D. E. (1991). Exon amplification: A strategy to isolate mammalian genes based on RNA splicing. *Proc. Natl. Acad. Sci. USA* **88:** 4005–4009.

Cheng, J.-F., Smith, C. L., and Cantor, C. R. (1989). Isolation and characterization of a human telomere. *Nucleic Acids Res.* **17:** 6109–6127.

Christian, C. L., Liner, R. I., Abu Bak'r, S., McCallum, W. D., and Conte, W. J. (1993). Genomic imprinting and the Beckwith–Wiedemann Syndrome associated with a familial chromosome 11 inversion. *Am. J. Hum. Genet.* **53:** 533.

Coppes, M. J., Bonetta, L., Huang, A., Hoban, P., Chilton-MacNeill, S., Campbell, C. E., Weksberg, R., Yeger, H., Reeve, A. E., and Williams, B. R. G. (1992). Loss of heterozygosity mapping in Wilms' tumor indicates the involvement of three distinct regions and a limited role for nondysjunction or mitotic recombination. *Genes Chrom. Cancer* **5:** 326–334.

Couillin, P., Le Guern, E., Vignal, A., Fizames, C., Ravisé, N., Delportes, D., Reguigne, I., Rosier, M. F., Junien, C., Van Heyningen, V., and Weissenbach, J. (1994). Assignment of 112 microsatellite markers to 23 chromosome 11 subregions delineated by somatic hybrids: Comparison with the genetic map. *Genomics* **21:** 379–387.

Davis, L. M., Byers, M. G., Fukushima, Y., Qin, S., Nowak, N. J., Scoggin, C., and Shows, T. B. (1988). Four new DNA markers are assigned to the *WAGR* region of 11p13: Isolation and regional assignment of 112 chromosome 11 anonymous DNA segments. *Genomics* **3:** 264–271.

Dowdy, S. F., Fasching, C. L., Araujo, D., Lai, K.-M., Livanos, E., Weissman, B. E., and Stanbridge, E. J. (1991). Suppression of tumorigenicity in Wilms' tumor by the p15.5–p14 region of chromosome 11. *Science* **254:** 293–295.

Feinberg, A. P., and Vogelstein, B. (1983). A technique for radiolabeling DNA restriction endonuclease fragments to high specific activity. *Anal. Biochem.* **132:** 6–13.

Flejter, W. L., Barcroft, C. L., Guo, S.-W., Lynch, E. D., Boehnke, M., Chandrasekharappa, S., Hayes, S., Collins, F. S., Weber, B. L., and Glover, T. W. (1993). Multicolor FISH mapping with *Alu*-PCR-amplified YAC clone DNA determines the order of markers in the BRCA1 region on chromosome 17q12–q21. *Genomics* **17:** 624–631.

Gelernter, J., Kennedy, J. L., van Tol, H. H. M., Civelli, O., and Kidd, K. K. (1992). The D4 dopamine receptor (DRD4) maps to distal 11p close to HRAS. *Genomics* **13:** 208–210.

Gessler, M., Hameister, H., Henry, I. L., Junien, C., Brown, T., and Arnold, H. H. (1990). The human MyoD (Myf3) gene maps on the short arm of chromosome 11 but is not associated with the WAGR locus or the region for the Beckwith–Wiedemann syndrome. *Hum. Genet.* **86:** 135–138.

Giannoukakis, N., Deal, C., Paquette, J., Goodyear, C., and Polychronakos, C. (1993). Parental genomic imprinting of the human IGF2 gene. *Nature Genet.* **4:** 98–101.

Glaser, B., Chiu, K. C., Anker, R., Nestorowicz, A., Landau, H., Ben-Bassat, H., Shlomai, Z., Kaiser, N., Thornton, P. S., Stanley, C. A., Spielman, R. S., Gogolin-Ewens, K., Cerasi, E., Baker, L., Rice, J., Donis-Keller, H., and Permutt, M. A. (1994). Familial hyperinsulinism maps to chromosome 11p14–15.1, 30 cM centromeric to the insulin gene. *Nature Genet.* **7:** 185–188.

Glaser, T., Housman, D., Lewis, W. H., Gerhard, D., and Jones, C. (1989). A fine-structure deletion map of human chromosome 11p: Analysis of J1 series hybrids. *Somatic Cell Mol. Genet.* **15:** 477–501.

Gyapay, G., Morissette, J., Vignal, A., Dib, C., Fizames, C., Millasseau, P., Marc, S., Bernardi, G., Lathrop, M., and Weissenbach, J. (1994). The 1993–94 Généthon human genetic linkage map. *Nature Genet.* **7:** 246–339.

Hao, Y., Crenshaw, T., Moulton, T., Newcomb, E., and Tycko, B. (1993). Tumor-suppressor activity of H19 RNA. *Nature* **365:** 764–767.

Harrison-Lavoie, K. J., John, R. M., Porteous, D. J., and Little, P. F. R. (1989). A cosmid clone map derived from a small region of human chromosome 11. *Genomics* **5:** 501–509.

Heding, I. J. J. P., Ivens, A. C., Wilson, J., Strivens, M., Gregory, S., Hoovers, J. M. N., Mannens, M., Redeker, B., Porteous, D., Van Heyningen, V., and Little, P. F. R. (1992). The generation of ordered sets of cosmid DNA clones from human chromosome region 11p. *Genomics* **13:** 89–94.

Henry, I., Bonaïti-Pellié, C., Chehensse, V., Beldjord, C., Schwartz, C., Utermann, G., and Junien, C. (1991). Uniparental disomy in a genetic cancer predisposing syndrome. *Nature* **351:** 665–667.

Henry, I., Grandjouan, S., Barichard, F., Huerre-Jeanpierre, C., and Junien, C. (1989). Mitotic deletions of 11p15.5 in two different tumors indicate that the CALCA locus is distal to the PTH locus. *Cytogenet. Cell Genet.* **50:** 155–157.

Henry, I., Van Heyningen, V., Puech, A., Scrable, H., Augereau, P., Boehma, T., Rabbitts, R., Mannens, M., Rochefort, H., Jones, C., Cavenee, W., and Junien, C. (1993). Reassessment of breakpoints in chromosome 11p15. *Cytogenet. Cell Genet.* **62:** 52–53.

Higgins, M. J., Hansen, M. F., Cavenee, W. K., and Lalande, M. (1989). Molecular detection of chromosomal translocations that disrupt the putative retinoblastoma susceptibility locus. *Mol. Cell. Biol.* **9:** 1–5.

Higgins, M. J., Turmel, C., Noolandi, J., Newmann, P. E., and Lalande, M. (1990). Construction of the physical map for three loci in chromosome band 13q14: Comparison to the genetic map. *Proc. Natl. Acad. Sci. USA* **87:** 3415–3419.

Holmquist, G. P. (1992). Chromosome bands, their chromatin flavors, and their functional features. *Am. J. Hum. Genet.* **51:** 17–37.

James, M. R., Richard, C. W., III, Schott, J.-L., Yousry, C., Clark, K., Bell, J., Hazan, J., Dubay, C., Vignal, A., Agrapart, M., Imai, T., Nakamura, Y., Polymeropoulos, M., Weissenbach, J., Cox, D. R., and Lathrop, G. M. (1994). A radiation hybrid map of 506 STS markers spanning human chromosome 11. *Nature Genet.*, in press.

Julier, C., Hyer, R. N., Davies, J., Merlin, F., Soularue, P., Briant, L., Cathelineau, G., Deschamps, I., Rotter, J. I., Froguel, P., Boltard, C., Bell, J. I., and Lathrop, G. M. (1991). Insulin-IGF2 region on chromosome 11p encodes a gene implicated in HLA-DR4-dependent diabetes susceptibility. *Nature* **354:** 155–159.

Junien, C., and Van Heyningen, V. (1991). Report of the committee on the genetic constitution of chromosome 11. *Cytogenet. Cell Genet.* **58:** 459–554.

Kao, F. T., Jones, C., and Puck, T. T. (1976). Genetics of somatic mammalian cells: Genetic, immunologic and biochemical analysis

with Chinese hamster cell hybrids containing selected human chromosomes. *Proc. Natl. Acad. Sci. USA* **73:** 193–197.

Keating, M., Atkinson, D., Dunn, C., Timothy, K., Vincent, G. M., and Leppert, M. (1991). Linkage of a cardiac arrhythmia, the long QT syndrome, and the Harvey ras-1 gene. *Science* **252:** 704–706.

Koi, M., Johnson, L. A., Kalikin, Little, P. F. R., Nakamura, Y., and Feinberg, A. P. (1993). Tumor cell growth arrest caused by subchromosomal transferable DNA fragments from chromosome 11. *Science* **260:** 361–364.

Koufos, A., Grundy, P., Morgan, K., Aleck, K. A., Hadro, T., Lampkin, B. C., Kalbakji, A., and Cavenee, W. K. (1989). Familial Wiedemann–Beckwith syndrome and a second Wilms' tumor locus both map to 11p15.5. *Am. J. Hum. Genet.* **44:** 711–719.

Lalande, M., Noolandi, J., Turmel, C., Rousseau, J., and Slater, G. W. (1987). Pulsed-field electrophoresis: Application of a computer model to the separation of large DNA molecules. *Proc. Natl. Acad. Sci. USA* **84:** 8011–8015.

Litt, M., Kramer, P., Hauge, X. Y., Weber, J. L., Wang, Z., Wilkie, P. J., Holt, M. S., Mishra, S., Donis-Keller, H., Warnich, L., Retief, A. E., Jones, C., and Weissenbach, J. (1993). A microsatellite-based index map of human chromosome 11. *Hum. Mol. Genet.* **2:** 909–913.

Loh, W. E., Jr., Scrable, H. J., Livanos, E., Arboleda, M. J., Cavenee, W. K., Oshimura, M., and Weissman, B. E. (1992). Human chromosome 11 contains two different growth suppressor genes for embryonal rhabdomyosarcoma. *Proc. Natl. Acad. Sci. USA* **89:** 1755–1759.

Mannens, M., Hoovers, J. M., Redeker, B., Bliek, J., Feinberg, A. P., Boavida, M., Tommerup, M., Henry, I., Little, P., Leschot, N. J., and Westerveld, A. (1991). Characterization of the region on human chromosome 11p involved in the development of Wilms' tumor associated congenital diseases: A model to study genomic imprinting in man. Eleventh international workshop on human gene mapping, London. *Cytogenet. Cell Genet.* **58:** 1967.

Morton, N. E. (1991). Parameters of the human genome. *Proc. Natl. Acad. Sci. USA* **88:** 7474–7476.

Moss, P. A. H., Davies, K. E., Boni, C., Mallet, J., and Reeders, S. T. (1986). Linkage of tyrosine hydroxylase to four other markers on the short arm of chromosome 11. *Nucleic Acids Res.* **14:** 9927–9933.

Newsham, I., Claussen, U., Ludecke, H.-J., Mason, M., Senger, G., Horsthemke, B., and Cavenee, W. (1991). Microdissection of chromosome band 11p15.5: Characterization of probes mapping distal to the HBBC locus. *Genes Chrom. Cancer* **3:** 108–116.

NIH/CEPH Collaborative Mapping Group (1992). A comprehensive genetic linkage map of the human genome. *Science* **258:** 67–86.

Norman, A. M., Read, A. P., Clayton-Smith, J., Andrews, T., and Donnai, D. (1992). Recurrent Wiedemann–Beckwith syndrome with inversion of chromosome (11)(p11.2p15.5). *Am. J. Med. Genet.* **42:** 638–641.

Ogawa, O., Becroft, D. M., Morison, I. M., Eccles, M. R., Skeen, J. E., Mauger, D. C., and Reeve, A. E. (1993). Constitutional relaxation of insulin-like growth factor II gene imprinting associated with Wilms' tumor and gigantism. *Nature Genet.* **5:** 408–412.

Ohlsson, R., Nyström, A., Pfeifer-Ohlsson, S., Tröhönen, V., Hedborg, F., Schofield, P., Flam, F., and Ekström, T. J. (1993). IGF2 is parentally imprinted during human embryogenesis and in the Beckwith–Wiedemann syndrome. *Nature Genet.* **4:** 94–97.

O'Rahilly, S., Patel, P., Lehmann, O. J., Tybjaerg-Hansen, A., Nerup, J., Turner, R. C., and Wainscoat, J. S. (1992). Multipoint linkage analysis of the short arm of chromosome 11 in non-insulin dependent diabetes including maturity onset diabetes of youth. *Hum. Genet.* **89:** 207–212.

Petronis, A., Van Tol, H. H. M., Lichter, J. B., Livak, K. J., and Kennedy, J. L. (1993). The D4 dopamine receptor gene maps on 11p proximal to HRAS. *Genomics* **18:** 161–163.

Ping, A. J., Reeve, A. F., Law, D. J., Young, M. R., Boehnke, M., and Feinberg, A. P. (1989). Genetic linkage of Beckwith–Wiedemann syndrome to 11p15. *Am. J. Hum. Genet.* **44:** 720–723.

Puech, A., Ahnine, L., Ludecke, H. J., Senger, G., Ivens, A., Jeanpierre, C., Little, P., Horsthemke, B., Claussen, U., Jones, C., Junien, C., and Henry, I. (1992). 11p15.5-specific libraries for identification of potential gene sequences involved in Beckwith–Wiedemann syndrome and tumorigenesis. *Genomics* **13:** 1274–1280.

Rainier, S., Johnson, L. A., Dobry, C. J., Ping, A. J., Grundy, P. E., and Feinberg, A. P. (1993). Relaxation of imprinted genes in human cancer. *Nature* **362:** 747–749.

Richard, C. W., III, Boehnke, M., Berg, D., Lichy, J. H., Meeker, T. C., Hauser, E., Myers, R. M., and Cox, D. R. (1993). A radiation hybrid map of the distal short arm of human chromosome 11 containing the Beckwith–Wiedemann and associated embryonal tumor disease loci. *Am. J. Hum. Genet.* **56:** 915–921.

Sait, S. N. J., Nowak, N. J., Singh-Kahlon, P., Weksberg, R., Squire, J., Shows, T. B., and Higgins, M. J. (1994). Localization of Beckwith–Wiedemann and rhabdoid tumor chromosome rearrangements to a defined interval in chromosome band 11p15.5. *Genes Chrom. Cancer,* in press.

Sanford, J., Kim, B.-W., Deaven, L. L., Jones, C., Higgins, M. J., Nowak, N. J., and Shows, T. B. (1993). A human chromosome 11 *Not*I end clone library. *Genomics* **15:** 653–658.

Schneider, R., Higgins, M. J., Kieninger, D., Schneider-Scherzer, E., Hirsch-Kauffmann, M., Schweiger, M., Eddy, R. L., Shows, T. B., and Zabel, B. U. (1992). The human ribonuclease/angiogenin inhibitor is encoded by a gene mapped to the chromosome 11p15.5 region, within 90 kb of the HRAS protooncogene. *Cytogenet. Cell Genet.* **59:** 264–267.

Schneider, R., Schneider-Scherzer, E., Thurnher, M., Aner, B., and Schweiger, M. (1988). The primary structure of human ribonuclease/angiogenin inhibitor (RAI) discloses a novel highly diversified protein super family with a common repetitive module. *EMBO J.* **7:** 415–416.

Scrable, H. J., Witte, D. P., Lampkin, B. C., and Cavenee, W. K. (1987). Chromosomal localization of the human rhabdomyosarcoma locus by mitotic recombination mapping. *Nature* **329:** 645–647.

Seizinger, B., Klinger, H. P. J., Junien, C., Nakamura, Y., LeBeau, M., Cavenee, W., Emmanuel, B., Ponder, B., Naylor, S., Mittelman, F., Louis, D., Menon, A., Newsham, I., Decker, J., Knelbling, M., Henry, I., and Deimling, A. V. (1991). Report of the committee on chromosome and gene loss in human neoplasia. *Cytogenet. Cell Genet.* **58:** 1080–1096.

Smith, R. J. H., Lee, E. C., Kimberling, W. J., Daiger, S. P., Pelias, M. Z., Keats, B. J. B., Jay, M., Bird, A., Reardon, W., Guest, M., Ayyagari, R., and Hejtmancik, F. (1992). Localization of two genes for Usher Syndrome Type I to chromosome 11. *Genomics* **14:** 995–1002.

Takiia, K. I., Tanigami, A., Tokino, T., Jones, C., and Nakamura, Y. (1992). Identification of 57 conventional RFLP and 6 VNTR systems with 32 DNA clones on chromosome 11p15. *Genomics* **13:** 1296–1299.

Tanigami, A., Tokino, T., Takiguchi, S., Mori, M., Glaser, T., Park, J. W., Jones, C., and Nakamura, Y. (1992). Mapping of 262 DNA markers into 24 intervals on human chromosome 11. *Am. J. Hum. Genet.* **50:** 56–64.

Tokino, T., Takahashi, E., Mori, M., Tanigama, A., Glaser, T., Park, J. W., Jones, C., Hori, T., and Nakamura, Y. (1991). Isolation and mapping of 62 new RFLP markers on human chromosome 11. *Am. J. Hum. Genet.* **48:** 258–268.

Trask, B. J., Massa, H., Kenwrick, S., and Gitschier, J. (1991). Mapping of human chromosome Xq28 by two-color fluorescence in situ hybridization of DNA sequences to interphase cell nuclei. *Am. J. Hum. Genet.* **48:** 1–15.

Turleau, C., DeGrouchy, J., Chavin-Colin, F., Martelli, H., Vover, M., and Charias, R. (1984). Trisomy 11p15 and Beckwith–Wiedemann syndrome: A report of two cases. *Hum. Genet.* **67:** 219–221.

Waziri, M., Paril, S. R., Hanson, J. W., and Bartley, J. A. (1983). Abnormality of chromosome 11 in patients with features of Beckwith–Wiedemann syndrome. *J. Pediatr.* **102:** 873–876.

Weissenbach, J., Gyapay, G., Dib, C., Vignal, A., Morissette, J., Milasseau, P., Vaysseix, G., and Lathrop, M. (1992). A second-generation linkage map of the human genome. *Nature* **359:** 794–801.

Weksberg, R., Teshima, I., Williams, B. R. G., Greenberg, C. R., Pueschel, S. M., Chernos, J. E., Fowlow, S. B., Hoyme, E., Anderson, I. J., Whiteman, D. A. H., Fisher, N., and Squire, J. (1993a). Molecular characterization of cytogenetic alterations associated with the Beckwith–Wiedemann syndrome (BWS) phenotype refined the localization and suggests the gene for BWS is imprinted. *Hum. Mol. Genet.* **2:** 549–556.

Weksberg, R., Shen, D. R., Fei, Y. L., Song, Q. L., and Squire, J. (1993b). Disruption of insulin-like growth factor 2 imprinting in Beckwith–Wiedemann syndrome. *Nature Genet.* **5:** 143–149.

Wiedemann, H.-R. (1964). Complexe maliformatif familial avec hernia obilicale et macroglossie. Un "syndrome nouveau"? *J. Genet. Hum.* **13:** 223–225.

Wiedemann, H.-R. (1983). Tumors and hemihypertrophy associated with Wiedemann–Beckwith syndrome. *Eur. J. Pediatr.* **141:** 129.

Winqvist, R., Mannermaa, A., Alavaikko, M., Blanco, G., Taskinen, P. J., Kiviniemi, H., Newsham, I., and Cavenee, W. (1993). Refinement of regional loss of heterozygosity for chromosome 11p15.5 in human breast tumors. *Cancer Res.* **53:** 4486–4488.

Xue, F., Kidd, J. R., Pakstis, A. J., Castiglione, C. M., Mallet, J., and Kidd, K. K. (1988). Tyrosine hydroxylase maps to the short arm of chromosome 11 proximal to the insulin and HRAS1 loci. *Genomics* **2:** 288–293.

Zhang, Y., and Tycko, B. (1992). Monoallelic expression of the human H19 gene. *Nature Genet.* **1:** 40–44.